

## ***In vivo* Transcription Analysis of Seabream Iridovirus (RSIV) Using DNA Microarrays**

DANG T. LUA<sup>1,2</sup>, IKUO HIRONO<sup>2</sup>, HIDEHIRO KONDO<sup>2</sup>  
and TAKASHI AOKI<sup>2</sup>

<sup>1</sup>*Aquatic Animal Disease Department, Centre for Environment  
and Disease Monitoring in Aquaculture (CEDMA), Research Institute for  
Aquaculture No.1 (RIA 1) Dinhbang - Tuson - Bacninh – Vietnam*

<sup>2</sup>*Laboratory of Genome Science, Graduate School of Marine Science and  
Technology Tokyo University of Marine Science and Technology  
Konan 4-5-7, Minato, Tokyo 108-8477, Japan*

### **ABSTRACT**

Red seabream iridovirus (RSIV) is the causative agent of an infectious disease in marine fish that is listed to be notifiable to the Office International des Epizooties. To better understand the molecular mechanisms of its pathogenesis, we explored the expression of almost all the putative RSIV open reading frames (ORFs) over the time-course of an *in vivo* infection in red seabream using DNA microarrays. Expression of about 45% of total RSIV ORFs was detected at about 5 days post-infection (d.p.i.). Almost all the ORFs (97% to 99%) were expressed at their maximum levels during the period 7-9 days post-infection (dpi). The expression levels and the number of expressed ORFs started to decrease at 10 dpi. Our results suggest that the pathogenesis of RSIV infection began at around day 5, and continued with high levels of viral multiplication until viral clearance, apparently by the host antiviral immune defenses, starting from around 10 dpi. RSIV ORFs were preferentially expressed in the spleen, which may be the primary target of RSIV. The spleen may thus be a susceptible organ for diagnosis of iridoviral disease in fish.

---

Lua, D. T., Hirono, I., Kondo, H. and Aoki, T. 2008. *In vivo* transcription analysis of seabream iridovirus (RSIV) using DNA microarrays, pp. 205-220. *In* Bondad-Reantaso, M.G., Mohan, C.V., Crumlish, M. and Subasinghe, R.P. (eds.). *Diseases in Asian Aquaculture VI*. Fish Health Section, Asian Fisheries Society, Manila, Philippines. 505 pp.

Corresponding author: Prof. Takashi Aoki: aoki@s.kaiyodai.ac.jp

## INTRODUCTION

Systemic iridoviral diseases have been observed in more than 100 freshwater and marine fish species worldwide with high mortalities ranging from 30% to 100% (Hyatt *et al.*, 2000; Iwamoto *et al.*, 2002; Qin *et al.*, 2003; Tidona *et al.*, 1998). One of these infectious diseases is red seabream iridoviral disease (RSIVD) that has been recorded in at least 31 marine fish species (Kawakami and Nakajima, 2002). The causative pathogen was first isolated from diseased red seabream (*Pagrus major*) in Japan in 1992 and hence named red seabream iridovirus (RSIV) (Inouye *et al.*, 1992). Because of geographical range and occurrence in fish involved in international trade, the RSIVD is notified to be quarantined by the Office International des Epizooties (OIE).

RSIV-infected fish showed diseased symptoms from 5 days of infection, and mortality commenced at day 6 and increased up to 90% at day 9 (Oshima *et al.*, 1998). The infected fishes displayed enlarged cells in spleen, kidney, liver and gills (Inouye *et al.*, 1992). Although some rapid, sensitive diagnostic methods, and control strategies have been developed (Caipang *et al.*, 2004; Caipang *et al.*, 2003; Caipang *et al.*, 2006; Jeong *et al.*, 2004; Kurita *et al.*, 1998; Nakajima *et al.*, 1995; Oshima *et al.*, 1998; Oshima *et al.*, 1996), the molecular mechanisms of its pathogenesis are poorly understood. Recently, the whole RSIV genomic sequence of about 112 kbp has been determined (Kurita *et al.*, 2002), providing an important basis for studies on its pathogenicity at the molecular level both *in vitro* and *in vivo*. *In vitro* expression analyses of individual viral genes at various time points during the viral life cycle can provide a better understanding of the viral DNA replication and gene expression strategies, while *in vivo* genome-wide transcription analyses can provide possible clues for the pathogenesis of the virus, and provide insights into the complex host-virus interactions (DeFilippis *et al.*, 2003; Martinez-Guzman *et al.*, 2003; Ye *et al.*, 2001).

The potential use of DNA microarray technology in virology has been comprehensively discussed in numerous reviews (Clewley, 2004; Cummings and Relman, 2000; DeFilippis *et al.*, 2003; Ye *et al.*, 2001). This technology is well suited for genome-wide transcription studies, and has been applied to explore gene expression patterns of viruses by both cell culture and animal model studies (see Lua *et al.*, 2005 and references therein). In a previous study (Lua *et al.*, 2005), we used DNA microarrays to monitor the *in vitro* transcription program of RSIV over the time-course of an infection. Individual RSIV ORFs were characterized at the transcriptional level and were also classified into temporal kinetic classes by their dependence on *de novo* protein synthesis and viral DNA replication. The gene expression of RSIV occurred in a temporal kinetic cascade with 3 stages, which includes Immediate-Early (IE), Early (E) and Late (L) transcripts, following a common feature of the family *Iridoviridae*. IE genes are expressed immediately after primary infection and encode transcription factors associated with *trans*-activations. E genes are normally expressed later and include enzymes associated with DNA replication. L genes are expressed after the onset of viral DNA replication and encode mainly structural proteins of viral particles. In the present study, we aimed to have a better understanding of the RSIV pathogenic mechanisms at the molecular level by monitoring the viral transcription profiles over the time-course of an *in vivo* infection in a fish model through the use of RSIV DNA microarrays.

## MATERIALS AND METHODS

### Virus stock

RSIV was obtained from a spleen homogenate of RSIV-infected red seabream, and propagated in Grunt fin (GF) cells (Clem *et al.*, 1961) as previously described (Lua *et al.*, 2005). The virus titer was determined using the 50% tissue culture infective dose (TCID<sub>50</sub>) method (Reed and Muench, 1938). The viral stock was stored in 1 ml aliquots at -80°C until further use.

### *In vivo* virus infection and time-course sampling

Red seabream juveniles were experimentally infected with 150 µl of the RSIV inoculum ( $5.0 \times 10^5$  TCID<sub>50</sub>/ml) and held in tanks supplied with running seawater at 25°C. Control fishes were injected with the same volume of phosphate buffered saline. Thirty fishes were sacrificed immediately after the RSIV infection for use as reference (control) samples. These fish are referred to as 0 day post-infection (dpi) fish. Five fish were randomly selected from the experimental population on each of 2, 3, 5, 7, 9, 10, and 14 dpi for use as target (test) samples. The spleens and kidneys were removed from the collected fish and stored in RNAlater (Ambion, USA) according to the manufacturer's protocol.

### Construction of RSIV DNA microarray chip

The DNA microarray chips containing almost all the putative RSIV open reading frames (ORFs) (92 ORFs) were constructed exactly as described by Lua *et al.* (2005). Briefly, specific primer sets were designed to amplify approximately 300-1500bp fragments of each ORF using viral genome as a template. All PCR products showing a single band of the appropriate size by gel electrophoresis were purified, and reconstituted in TE buffer at a final concentration of about 500 µg/ml for spotting onto the glass slides. Each ORF was spotted in duplicate at different parts of the slides to assess the consistency of hybridization and facilitate comparison during the analysis. Piscine β-actin genes from Japanese flounder, red seabream, and Japanese flounder natural embryo (HINAE) cells (Kasai and Yoshimizu, 2001) were included as internal controls to normalize the microarray data. In addition, distilled water was also used as a negative control.

### Microarray hybridization experiment

Total RNA was extracted from the collected spleens with TRIzol (Invitrogen, USA) and subjected to DNase I treatment (Promega, USA) according to the manufacturer's protocols. For each time-course target sample and control sample, cDNAs were generated from 50 µg total RNA using an RSIV antisense-strand specific primer mixture. The cDNAs were first labeled with aminoallyl-dUTP using a LabelStar™ Array Kit (Qiagen, USA) and purified with a QIAquick PCR Purification Kit (Qiagen, USA) following the manufacturer's recommendations. The target and control aminoallyl-cDNAs were then

coupled with Cy5- and Cy3-monofunctional dyes (Amersham Biosciences, England), respectively, and purified with MinElute™ Spin columns (Qiagen, USA) according to manufacturer's instructions.

At each indicated time point, the Cy5/Cy3-dUTP labeled cDNAs were combined and hybridized to the microarray chips for 16-18h at 42°C. The chips were rinsed several times and finally dried following the DNA microarray standard method (Bowtell and Sambrook, 2002) as modified by Lua *et al.* (2005).

### **Microarray statistical data analysis**

The microarray chips were scanned using a GenePix 4000B array scanner and images were analyzed by GenePix Pro 4.0 array analysis software (Axon Instruments, Inc., USA). The Cy5 and Cy3 signal intensities of viral genes were normalized to the signal intensities of the spotted  $\beta$ -actin gene. The background signal was subtracted from the median signal intensity to obtain the absolute viral gene expression. Only genes exhibiting signal intensity at least twofold greater than the signal intensities of the reference samples collected at 0 d.p.i. were used for statistical analysis. The significance of differences between viral infected samples and reference samples was determined with a paired *t*-test on replicated spots for each gene. *P* values of less than 0.05 were considered significant.

The microarray data was also reported as the calibrated expression ratio, which was the ratio of the fluorescence intensity of a RSIV transcript in infected spleens compared to that of the  $\beta$ -actin transcript (Lua *et al.*, 2005; Tsai *et al.*, 2004). The expression ratio data was imported into the cluster program 3.0 in conjunction with an average linkage hierarchical clustering algorithm using Euclidian distance as the similarity metric. After clustering, the results were visualized in a tree structure by using a tree view program (Eisen *et al.*, 1998).

### **Reverse Transcription (RT) - PCR**

RT-PCR assay was used to confirm the microarray data and to investigate a susceptible organ of RSIV infection. Several RSIV ORFs, with different expression patterns as determined by the microarray results, were selected from the three temporal kinetic classes (IE, E and L genes). Twenty  $\mu$ l of cDNA was synthesized from 5  $\mu$ g total RNA derived from spleens and kidneys by using M-MLV Reverse Transcriptase (Invitrogen, USA) according to the manufacturer's protocols. RT-PCR was carried out in a 30  $\mu$ l reaction volume containing 1  $\mu$ l cDNA using Taq polymerase. The same specific primers for each RSIV ORF used in the amplification of microarray probes were also employed here. Cycling parameters consisted of an initial denaturation at 95°C for 2 min, followed by 23 and 27 cycles of denaturation at 95°C for 30 sec, annealing at 55°C for 30 sec and elongation at 72°C for 1 min, and a final elongation step at 72°C for 5 min. A 23 cycle PCR was used to determine differences in expression of RSIV transcripts between spleen and kidney at the high level spread stage of the infection (7-9 dpi) while a 27 cycle PCR was performed to show differences in expression at the early stage (5 dpi) and late stage (10-14 dpi) of the infection.

## RESULTS

### ***In vivo* RSIV transcription program**

The microarray analysis showed that no viral transcripts were detected in spleens at 2 and 3 dpi (data not shown), but viral ORFs showed significant changes in expression from 5 d.p.i. onwards. At 5 days after infection, 44 viral ORFs were significantly expressed, accounting for 44.6% ( $p < 0.05$ ) of total RSIV ORFs. Almost all (about 97% to about 99%,  $p < 0.001$ ) of viral ORFs were significantly expressed during the period 7-9 dpi (Table 1). As shown by the cluster analysis (Figure 1), the expression levels of viral ORFs were at their maximal levels during this period, showing high levels of viral multiplication. However, the numbers and the expression levels of expressed ORFs started to decrease at 10 dpi. The expression of only 25% ( $p < 0.05$ ) of the ORFs was detected at 14 dpi (Table 1, Figure 1).

### **Confirmation of microarray results by RT-PCR**

Six RSIV ORFs were selected for confirming the microarray results by RT-PCR (Fig. 2). These ORFs included IE transcripts 097R and 591R, E transcripts 092R and 324R, and L transcripts 291L and MCP (Major Capsid Protein). The  $\beta$ -actin transcript was used as an internal control. As expected, no viral band was amplified at day 0, day 2 or day 3 of the infection. From 5 d.p.i. onwards, the selected ORFs were observed with different expression levels over the time-course of the infection. Therefore, the RT-PCR results (Figure 2) confirmed the microarray data showing the same expression patterns of selected ORFs. In addition, the  $\beta$ -actin transcript levels, as determined by RT-PCR, were similar between samples, confirming that the  $\beta$ -actin gene can be used to normalize the viral gene expression results across the microarrays.

### **Identification of a susceptible organ of RSIV infection**

Four ORFs were selected for identifying a susceptible organ of RSIV infection by RT-PCR (Figure 3). These ORFs consisted of IE transcript 097R, E transcript 407R, and L transcripts 291L and MCP. Differences in expression of these ORFs between spleens and kidneys during the spreading stage of the virus (7-9 dpi) were detected after both 23 and 27 PCR cycles (Figures 3A and 3B), while the differences at the early stage (5 dpi) and the late stage (10-14 dpi) of the infection were detected after 27 PCR cycles (Figure 3B). The expression levels of the selected ORFs were all higher in the spleen than in the kidney. These findings indicate that the spleen may be a susceptible organ of RSIV infection.

**Table 1.** Microarray analysis of in vivo RSIV transcription program.

No.	ORF	Putative Function	Accession No.	Signal Intensity Value <sup>a</sup>			Calibrated Expression Ratio <sup>b</sup>			Kinetic class <sup>c</sup>			
				5 d.p.i.	7 d.p.i.	9 d.p.i.	5 d.p.i.	7 d.p.i.	9 d.p.i.		10 d.p.i.	14 d.p.i.	
1	ORF016L	Hypothetical protein		430	1287	728	135	0.45	2.38	1.61	0.23		L
2	ORF018R	Hypothetical protein			1177	1398	362		2.18	3.09	0.63		L
3	ORF029R	Hypothetical protein			480	209			0.89	0.46			ND
4	ORF033R	Cytosine DNA methyltransferase	AAT71861		223	157	153		0.41	0.35	0.27		E
5	ORF037R	Hypothetical protein		560	2103	1586	506	0.59	3.89	3.51	0.88		L
6	ORF042R	Hypothetical protein		1370	5346	1650	404	1.44	9.90	3.65	0.70	0.14	L
7	ORF049R	RING-finger-containing E3 ubiquitin ligase	AAT71876	192	2212		293	0.20	4.10		0.51	0.13	IE
8	ORF054R	Putative RNA guanyltransferase	AAAL98788		242	116	127		0.45	0.26	0.22		E
9	ORF063R	Subunit of DNA-dependent RNA polymerase	BAA82753		505	207			0.94	0.46			E
10	ORF077R	Putative DNA-binding protein	AAT71873		746	492	258		1.38	1.09	0.45		E
11	ORF092R	Putative replication factor	AAAS18131	117	3126	938	843	0.12	5.79	2.08	1.47	0.16	E
12	ORF097R	Hypothetical protein		471	11601	8886	5031	0.50	21.48	19.66	8.75	0.44	IE
13	ORF101R	Hypothetical protein			1115	1318	627		2.06	2.92	1.09	0.13	L
14	ORF106R	Hypothetical protein		135	1783	1384	1312	0.14	3.30	3.06	2.28	0.30	L
15	ORF111R	Hypothetical protein		804	13835	6500	4051	0.85	25.62	14.38	7.05	0.52	L
16	ORF122R	Hypothetical protein			513	608	301		0.95	1.35	0.52		L
17	ORF128R	Hypothetical protein		90	763	1219	291		1.41	2.70	0.51		E
18	ORF135L	Hypothetical protein			847	1415	802	0.09	1.57	3.13	1.39		L
19	ORF140R	Cytosine DNA methyltransferase	AAT71861		530	472	158		0.98	1.04	0.27		ND
20	ORF145R	Hypothetical protein			820	565	259		1.52	1.25	0.45		E
21	ORF151R	Hypothetical protein			387	311	169		0.72	0.69	0.29		E
22	ORF156R	Thiol oxidoreductase	AAAP33193		268	232	118		0.50	0.51	0.21		E
23	ORF161L	Hypothetical protein			471	349			0.87	0.77			E
24	ORF162R	Hypothetical protein			368	269	170		0.68	0.60	0.30		E
25	ORF171R	Hypothetical protein			684	289	144		1.27	0.64	0.25		E
26	ORF179L	Hypothetical protein			223	157	180		0.41	0.35	0.31		E
27	ORF180R	Hypothetical protein		138	1171	584	187	0.15	2.17	1.29	0.33		ND
28	ORF186R	Hypothetical protein			300	283	139		0.56	0.63	0.24		L
29	ORF197L	Hypothetical protein		119	2377	1047	460	0.13	4.40	2.32	0.80	0.18	L
30	ORF198R	Hypothetical protein			197		108		0.36		0.19		E
31	ORF224L	RNA polymerase beta subunit	AAT71848		584	390	112		1.08	0.86	0.19		L
32	ORF226R	Hypothetical protein		263	501	767	216	0.28	0.93	1.70	0.38		L
33	ORF234L	Deoxyribonucleoside kinase	AAT71846		150	191			0.28	0.42			E
34	ORF237L	Subunit of DNA-dependent RNA polymerase	AB018418		896	626			1.66	1.39			E
35	ORF239R	Subunit of DNA-dependent RNA polymerase	BAA82753		561	427	118		1.04	0.94	0.21		E

Table 1. (continued)

No.	ORF	Putative Function	Accession No.	Signal Intensity Value <sup>a</sup>			Calibrated Expression Ratio <sup>b</sup>					Kinetic class <sup>c</sup>
				5 d.p.i.	7 d.p.i.	9 d.p.i.	5 d.p.i.	7 d.p.i.	9 d.p.i.	10 d.p.i.	14 d.p.i.	
36	ORF256R	DNA repair protein RAD2	BAA82754	1057	1174	507	1.96	2.60	0.88			L
37	ORF261R	Hypothetical protein		208	106		0.39	0.23				L
38	ORF268L	Ribonucleotide reductase small subunit	BAA82755	762	818	333	1.41	1.81	0.58			E
39	ORF291L	Laminin-type epidermal growth factor-like domain	AAI71838	6859	1729	561	12.70	3.83	0.98	0.32		L
40	ORF317L	DNA polymerase	AB007366	963	405	120	1.78	0.90	0.21			E
41	ORF321R	DNA polymerase	AB007366	95	146		0.18	0.32				E
42	ORF324R	DNA polymerase	AB007366	870	707	415	1.61	1.56	0.72	0.29		E
43	ORF333L	Hypothetical protein		1396	870	513	2.59	1.92	0.89			IE
44	ORF342L	Hypothetical protein		1149	698	258	2.13	1.54	0.45			IE
45	ORF349L	Serine/threonine protein kinase catalytic domain	AAI71828	964	1909	766	1.79	4.22	1.33			L
46	ORF351R	Hypothetical protein		205	265	204	0.38	0.59				E
47	ORF353R	Hypothetical protein		668	766	465	1.24	1.69	0.81			IE
48	ORF373L	Hypothetical protein		1483	1164	367	2.75	2.58	0.64			L
49	ORF374R	Hypothetical protein		8571	6712	1752	15.87	14.85	3.05	0.11		L
50	ORF380R	Major capsid protein	BAC66968	1645	1464	1017	3.05	3.24	1.77	0.27		L
51	ORF385R	Catalytic domain of ctd-like phosphatase	AAI71821	411	459	204	0.76	1.02	0.35			E
52	ORF390R	Hypothetical protein		652	365		1.21	0.81				L
53	ORF394R	Hypothetical protein			215		0.48					L
54	ORF396R	Transmembrane amino acid transporter	AAI71816	1562	1084	401	2.89	2.40	0.70			IE
55	ORF401R	Hypothetical protein		611	780	251	1.13	1.73	0.44			L
56	ORF407R	ATPase	AB007367	5551	1952	671	10.28	4.32	1.17	0.28		E
57	ORF412L	ATPase	AAO16492	532	744	363	0.99	1.65	0.63	0.11		E
58	ORF413R	ATPase	AB007367	303	562	318	0.56	1.24	0.55			E
59	ORF420L	Hypothetical protein		854	362	113	1.58	0.80	0.20			L
60	ORF423L	RING-finger domain-containing protein	AAI71906	123	251		0.23	0.56				L
61	ORF424R	Putative ankyrin repeat protein	AAL98801	1673	786	213	3.10	1.74	0.37			E
62	ORF426R	Hypothetical protein	AAI71837	1947	983	835	3.61	2.17	1.45	0.85		L
63	ORF430L	Putative phosphatase		5175	1696	610	9.58	3.75	1.06	0.17		E
64	ORF458L	Hypothetical protein		5939	3039	952	11.00	6.72	1.66	0.20		L
65	ORF463R	Hypothetical protein	NP078615	707	507	120	1.31	1.12	0.21			L
66	ORF487L	Proliferating cell nuclear antigen	AAL98835	424	389	108	0.79	0.86	0.19			E
67	ORF488R	Putative tumor necrosis receptor associated-factor	AAS18067	308	277		0.57	0.61				L
68	ORF493R	D5 family NTPase		1244	642	215	2.30	1.42	0.37			L
69	ORF502R	Hypothetical protein		111	212		0.21	0.47				L
70	ORF506R	Hypothetical protein		395	313		0.73	0.69		0.20		L

Table 1. (continued)

No.	ORF	Putative Function	Accession No.	Signal Intensity Value <sup>a</sup>			Calibrated Expression Ratio <sup>b</sup>			Kinetic class <sup>c</sup>	
				5 d.p.i.	7 d.p.i.	9 d.p.i.	5 d.p.i.	7 d.p.i.	9 d.p.i.		10 d.p.i.
71	ORF515L	Hypothetical protein		92	171	106		0.17	0.23		ND
72	ORF522L	Hypothetical protein		101	111	230		0.21	0.51		L
73	ORF534L	Ankyrin repeat-containing protein	AAT71909	501	1434	1844	122	2.66	4.08	1.27	E
74	ORF535R	Hypothetical protein		388	5996	2862	222	11.10	6.33	2.28	IE
75	ORF543R	RING-finger domain-containing protein	AAT71906	95	4080	1732	202	0.41	7.56	1.30	L
76	ORF550R	Hypothetical protein		626	548	368	60	1.16	1.21	0.41	L
77	ORF554R	Hypothetical protein		1041	241	368		1.93	1.17	0.42	L
78	ORF562R	Hypothetical protein		103	705	470		1.31	1.04	0.33	E
79	ORF569R	Hypothetical protein		2386	1222	439		4.42	2.70	0.76	E
80	ORF575R	Hypothetical protein		463	385	209		0.86	0.85	0.36	L
81	ORF586L	Hypothetical protein		171	363	273		0.67	0.60		E
82	ORF589L	Hypothetical protein		85	873	674		1.62	1.49	0.69	E
83	ORF591R	Hypothetical protein	AAT71898	92	1199	830		2.22	1.84	0.39	IE
84	ORF596L	dsRNA-specific ribonuclease		283	311	128		0.52	0.69	0.22	L
85	ORF600L	Hypothetical protein		396	517	167		0.73	1.14	0.29	E
86	ORF606R	Hypothetical protein		258	363	125		0.48	0.80	0.22	L
87	ORF617L	Hypothetical protein		224	137	144		0.25	0.32		E
88	ORF618R	Hypothetical protein		277	1905	782	110	3.53	1.73	1.79	E
89	ORF628L	Hypothetical protein		139	4141	1203	122	0.29	7.67	0.63	E
90	ORF632L	Hypothetical protein		141	2143	708		0.15	3.97	1.23	IE
91	ORF635L	Hypothetical protein		1538	576	149		2.85	1.27	0.26	E
92	ORF641L	Putative ankyrin repeat protein	AAL98801	44.6*	98.9**	96.7**	25*	0.15			

<sup>a</sup>Signal intensity value is the background-subtracted median value

<sup>b</sup>The calibrated expression ratio is the ratio of the expression of the RSIV ORF in viral-infected cells compared to the  $\beta$ -actin control gene

<sup>c</sup>Abbreviation: IE, Immediate-Early; E, Early; L, Late; ND, Not Detected (adapted by Lua et al. 2005); \*( $p < 0.05$ ); \*\*( $p < 0.001$ )

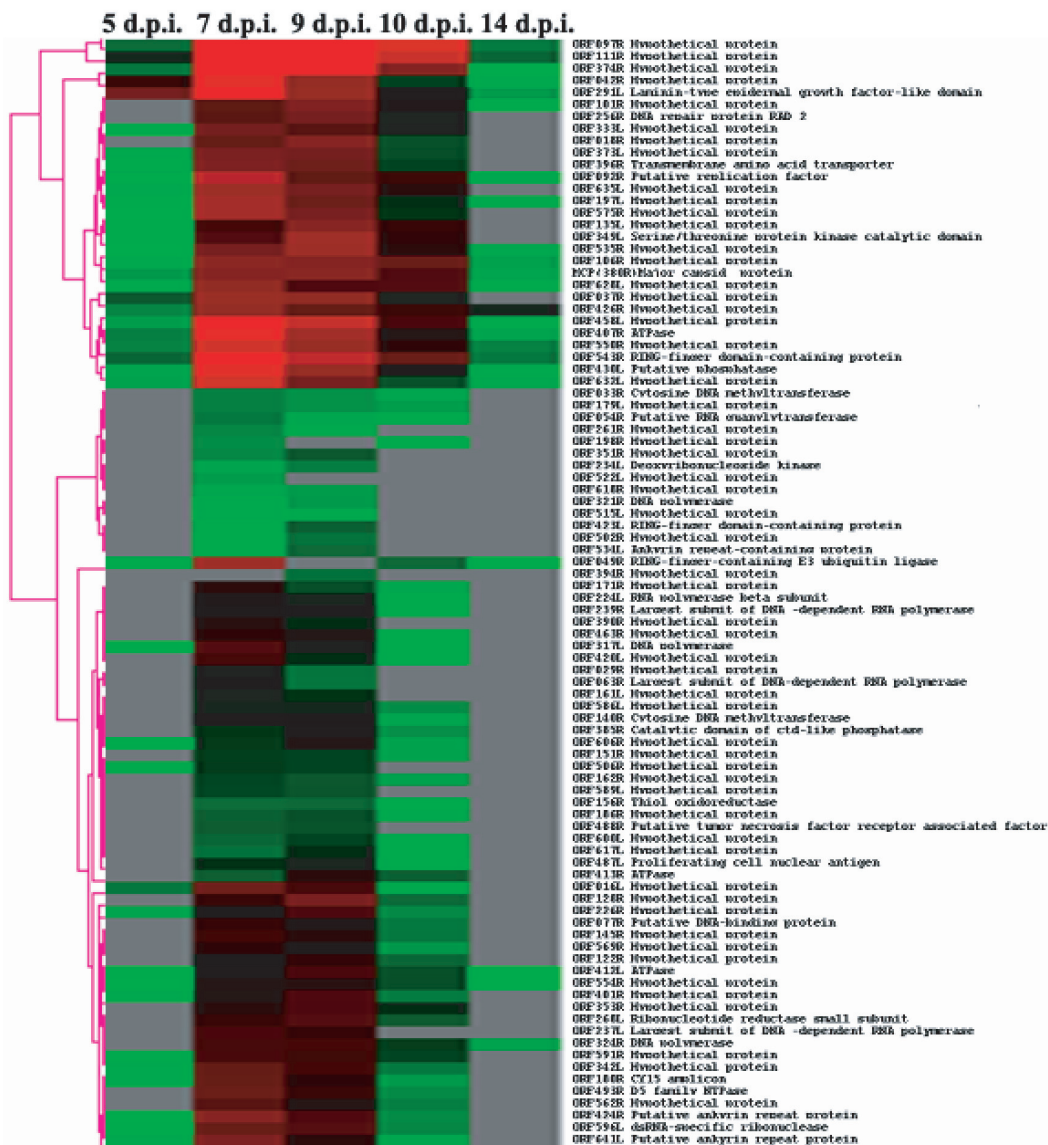


**Figure 1.** Hierarchical cluster analysis of *in vivo* RSIV transcription program. Calibrated expression ratios for each ORF were categorized by an average linkage hierarchical clustering program. Each row represents the expression profile of a single ORF, and each column indicates time points after infection. The normalized expression levels across all the time points are color-coded. Green boxes indicate expression ratios lower than the mean. Red boxes indicate expression ratios greater than the mean. Black boxes indicate an intermediate level of expression and gray boxes indicate missing or not detected. The magnitude of up-regulation from the mean is shown by differing intensities of red, with deep red showing lower expression and bright red showing the highest levels of expression.

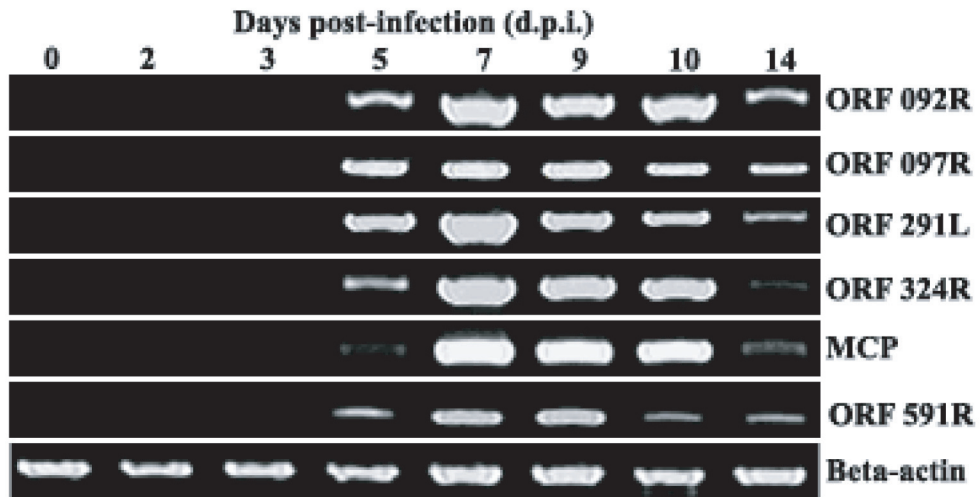


**Figure 2.** RT-PCR analysis of RSIV gene expression in viral-infected spleen. cDNAs were synthesized from 5 µg total RNA taken from the same samples used for the microarray experiments. One µl cDNA was used for 30 µl RT-PCR reaction with cycling conditions as follows: an initial denaturation at 95°C for 2 min, followed by 27 cycles of denaturation of 95°C for 30 sec, annealing at 55°C for 30 sec and elongation at 72°C for 1 min, and a final elongation step at 72°C for 5 min.



**Figure 3.** Difference in expression of RSIV genes between spleen (S) and kidney (K). cDNAs were synthesized from 5 µg total RNA derived from spleens and kidneys. One µl cDNA was used for 30 µl RT-PCR reaction with cycling conditions as follows: an initial denaturation at 95°C for 2 min, followed by 23 and 27 cycles of denaturation of 95°C for 30 sec, annealing at 55°C for 30 sec and elongation at 72°C for 1 min, and a final elongation step at 72°C for 5 min. A 23 cycle PCR was used to determine differences in expression of RSIV transcripts between spleen and kidney at the high level spread stage of the infection while a 27 cycle PCR was performed to show differences in expression at the early and late stages of the infection.

## DISCUSSION

Outbreaks of system iridoviral diseases associated with high mortality (30-100%) have been reported in cultured freshwater and marine fish species in many parts of the world including Africa, America, Asia, and Europe (Chao *et al.*, 2004; Iwamoto *et al.*, 2002; Qin *et al.*, 2003). Among them, an iridoviral disease caused by RSIV has been considered as a serious, important disease because of its wide geographical distribution and host range. The disease is documented not only in Japan, but also in Korea, Taiwan and Indonesia (Chao *et al.*, 2002; Chou *et al.*, 1998; Do *et al.*, 2004; Inouye *et al.*, 1992; Jeong *et al.*, 2003; Mahardika *et al.*, 2004; Wang *et al.*, 2003). In Japan, the disease has been recorded in at least 31 marine fish including 3 main cultured marine fish, red seabream, Japanese flounder and yellow tail (Kawakami and Nakajima, 2002). Due to the devastating effects of this pathogen to marine aquaculture, an understanding of RSIV pathogenic mechanism, at the molecular level, is necessary and may provide possible clues for disease control and diagnosis strategies.

The concurrent development of DNA microarray technology and the complete sequencing of a number of viral genomes are providing the opportunity to speed our understanding of various aspects of both sides of the host-virus interaction at the molecular level. In fact, the DNA microarray technology has been successfully applied in virological studies in both cell culture systems and experimental animal models. In our previous study (Lua *et al.*, 2005), RSIV DNA microarrays were used for rapid analysis of the RSIV gene transcriptional profile over the time-course of an *in vitro* infection in HINAE cells and for grouping genes into temporal kinetic classes, providing a global picture of transcription and kinetics of RSIV genes during the replication cycle. In the present study, the same RSIV DNA microarray was used to characterize the viral gene expression profiles over the time-course of an *in vivo* infection in red seabream, providing a better understanding of the pathogenic mechanisms of RSIV infection at the transcription level.

The time-course experiments have allowed us to monitor the expression of each RSIV ORF through an *in vivo* infection. The timing of viral transcripts that we observed (beginning at 5 dpi and peaking at 7-9 dpi) is similar to what has been observed in previous studies (Nakajima *et al.*, 1995; Oshima *et al.*, 1998). In an immunoassay of RSIV-infected red seabream (Nakajima *et al.*, 1995), the virus was not detected in the spleen at 1 or 3 dpi, was moderately detected at 5 dpi and was strongly detected at 7 dpi. Using a PCR assay, PCR products corresponding to a portion of the ribonucleotide reductase small subunit gene were not amplified from RSIV-infected red seabream at 1 and 2 dpi but were amplified starting at 5 dpi (Oshima *et al.*, 1998). Similar results were observed in Taiwan grouper iridovirus (TGIV) infection, a piscine iridovirus classified into the same group with RSIV, in which the viral particles were determined in some internal organs of groupers at 4-5 days after intramuscular infection (Chao *et al.*, 2002). In Singapore grouper iridovirus (SGIV) infection, viral antigens were detected in virus-infected fish blood at 3 dpi by a Western blot analysis (Qin *et al.*, 2002). Taken together, our results suggest that the pathogenic mechanism of RSIV is probably similar to that found in other piscine iridoviruses, such as TGIV and SGIV. Although viral particles were detected at slightly different times in the above studies, piscine iridoviruses seem to begin to spread at around 4-5 dpi.

Our finding that the *in vivo* expression profiles of RSIV gradually declined in both the numbers and the expression levels after 10 dpi. (Table 1, Fig. 1) indicates that the virus was being gradually cleared by host antiviral immune defenses. Similarly, Caipang *et al.* (2003) showed with real-time PCR that RSIV was cleared from both the vaccinated and unvaccinated red seabream after viral challenge, and Chao *et al.* (2004) showed with H & E staining and *in situ* hybridization that the number of basophilic enlarged cells (virus-containing cells) gradually decreased in groupers 7 days after TGIV infection. Chao *et al.* (2004) attributed the viral clearance to either an improved host defense or to depletion of susceptible cell types.

Differences in expression of selected RSIV ORFs between spleens and kidneys at high spread stage of the infection could be observed with only 23 PCR cycles (Figure 3A). Although differences in expression at the early and late stages of the infection were not detectable after 23 cycles, they were detectable after 27 cycles (Figure 3B). Overall, the expression levels of the selected ORFs were all higher in the spleen than in the kidney. Among the selected ORFs, the MCP gene was found to be expressed at significant higher levels in the spleen than in the kidney over the time-course of infection. MCP gene contains highly conserved domains and codes for the major structural component of viral particles (Schnitzler and Darai, 1993; Tidona *et al.*, 1998; Williams, 1996). The MCP gene has been used to detect and measure RSIV as well as other iridoviruses (Caipang *et al.*, 2003; Tidona *et al.*, 1998). Thus, our RT-PCR results confirmed, at the transcription level, the hypothesis that the spleen is a susceptible organ for RSIV infection in particular and for iridoviral infections in fish in general. The spleen also appears to be where TGIV begins replicating (Chao *et al.*, 2004), and thus has been suggested to be used for early screening of TGIV. Our results support this conclusion.

## CONCLUSION

In conclusion, the present study is the continued analysis of RSIV gene expression patterns *in vivo* to complete transcriptional profiles of RSIV both in cell culture and fish model systems. The results demonstrate that RSIV DNA microarrays can be used to study RSIV infection in a fish model at the molecular level. This study describes the first use of DNA microarrays to explore gene expression patterns of a marine fish-pathogenic virus in fish. Such studies should impart a greater understanding of pathogenesis of RSIV infection at the molecular level, contribution to the thorough knowledge of RSIV infection and further provide a possible clue for selection of a susceptible organ for detection of iridoviral infections in aquaculture.

## ACKNOWLEDGMENTS

The authors thank Dr. Jun Kurita of the Japanese National Research Institute of Aquaculture, Fisheries Research Agency, for providing genome information on RSIV.

This study was supported in part by a Grant-in-Aid for Scientific Research (S) from the Ministry of Education, Culture, Sports, Sciences and Technology of Japan.

## REFERENCES

- Bowtell, D. and Sambrook, J. (eds.). 2002. DNA microarrays: A Molecular Cloning Manual, New York.
- Caipang, C. M., Haraguchi, I., Ohira, T., Hirono, I. and Aoki, T. 2004. Rapid detection of a fish iridovirus using loop-mediated isothermal amplification (LAMP). *J. Virol. Methods* 121: 155-161.
- Caipang, C. M., Hirono, I. and Aoki, T. 2003. Development of a real-time PCR assay for the detection and quantification of red sea bream *Iridovirus* (RSIV). *Fish Path.* 38:1-7.
- Caipang, C. M., Hirono, I. and Aoki, T. 2006. Immunogenicity, retention and protective effects of the protein derivatives of formalin-inactivated red seabream iridovirus (RSIV) vaccine in red seabream, *Pagrus major*. *Fish Shellfish Immunol* 20:597-609.
- Chao, C. B., Chen, C. Y., Lai, Y. Y., Lin, C. S. and Huang, H. T. 2004. Histological, ultrastructural, and in situ hybridization study on enlarged cells in grouper *Epinephelus* hybrids infected by grouper iridovirus in Taiwan (TGIV). *Dis. Aquat. Org.* 58:127-142.
- Chao, C. B., Yang, S. C., Tsai, H. Y., Chen, C. Y., Lin, C. S. and Huang, H. T. 2002. A Nested PCR for the detection of grouper iridovirus in Taiwan (TGIV) in cultured hybrid grouper, giant seaperch, and largemouth bass. *J. Aquat. Anim. Health* 14:104-113.
- Chou, H. Y., Hsu, C. C. and Peng, T. Y. 1998. Isolation and characterization of a pathogenic iridovirus from cultured grouper (*Epinephelus* sp.) in Taiwan. *Fish Path.* 33:201-206.
- Clem, L. W., Moewus, L. and Sigel, M. M. 1961. Studies with cells from marine fish in tissue culture. *Proc. Soc. Exp. Biol. Med.* 108:762-766.
- Clewley, J. P. 2004. A role for arrays in clinical virology: fact or fiction? *J. Clin. Virol.* 29:2-12.
- Cummings, C. A. and Relman, D. A. 2000. Using DNA microarrays to study host-microbe interactions. *Emerg. Infect. Dis.* 6:513-525.
- DeFilippis, V., Raggio, C., Moses, A. and Fruh, K. 2003. Functional genomics in virology and antiviral drug discovery. *Trends in Biotechnol.* 21:452-457.
- Do, J. W., Moon, C. H., Kim, H. J., Ko, M. S., Kim, S. B., Son, J. H., Kim, J. S., An, E. J., Kim, M. K., Lee, S. K., Han, M. S., Cha, S. J., Park, M. S., Park, M. A., Kim, Y. C., Kim, J. W. and Park, J. W. 2004. Complete genomic DNA sequence of rock bream iridovirus. *Virol.* 325:351-363.
- Eisen, M. B., Spellman, P. T., Brown, P. O. and Botstein, D. 1998. Cluster analysis and display of genome-wide expression patterns. *Proc. Natl. Acad. Sci. USA* 95:14863-14868.
- Hyatt, A. D., Gould, A. R., Zupanovic, Z., Cunningham, A. A., Hengstberger, S., Whittington, R. J., Kattenbelt, J. and Coupar, B. E. 2000. Comparative studies of piscine and amphibian iridoviruses. *Arch. Virol.* 145:301-331.

- Inouye, K., Yamano, K., Maeno, Y., Nakajima, K., Matsuoka, M., Wada, Y. and Sorimachi, M. 1992. Iridovirus infection of cultured red sea bream, *Pagrus major*. *Fish Path.* 27:19-27.
- Iwamoto, R., Hasegawa, O., Lapatra, S. and Yoshimizu, M. 2002. Isolation and characterization of the Japanese flounder (*Paralichthys olivaceus*) lymphocystis disease virus. *J. Aquat. Anim. Health* 14:114-123.
- Jeong, J. B., Jun, L. J., Yoo, M. H., Kim, M. S., Komisar, J. L. and Jeong, H. D. 2003. Characterization of the DNA nucleotide sequences in the genome of red sea bream iridoviruses isolated in Korea. *Aquaculture* 220:119-133.
- Jeong, J. B., Park, K. H., Kim, H. Y., Hong, S. H., Kim, K. H., Chung, J. K., Komisar, J. L. and Jeong, H. D. 2004. Multiplex PCR for the diagnosis of red sea bream iridoviruses isolated in Korea. *Aquaculture* 235:139-152.
- Kasai, H. and Yoshimizu, M. 2001. Establishment of two Japanese flounder embryo cell lines. *Bull. Fisheries Sci. Hokkaido University* 52:67-70.
- Kawakami, H. and Nakajima, K. 2002. Cultured fish species affected by red sea bream iridoviral disease from 1996-2000. *Fish Path.* 37:45-47.
- Kurita, J., Nakajima, K., Hirono, I. and Aoki, T. 1998. Polymerase chain reaction (PCR) amplification of DNA of red sea bream iridovirus (RSIV). *Fish Path.* 33:17-23.
- Kurita, J., Nakajima, K., Hirono, I. and Aoki, T. 2002. Complete genome sequencing of red sea bream *Iridovirus* (RSIV). *Fish. Sci.* 68:1113-1115.
- Lua, D. T., Yasuike, M., Hirono, I. and Aoki, T. 2005. Transcription program of red sea bream iridovirus as revealed by DNA microarrays. *J. Virol.* 79:15151-15164.
- Mahardika, K., Zafran, Yamamoto, A. and Miyazaki, T. 2004. Susceptibility of juvenile humpback grouper *Cromileptes altivelis* to grouper sleepy disease iridovirus (GSDIV). *Dis. Aquat. Organ.* 59:1-9.
- Martinez-Guzman, D., Rickabaugh, T., Wu, T. T., Brown, H., Cole, S., Song, M. J., Tong, L. and Sun, R. 2003. Transcription program of murine gammaherpesvirus 68. *J. Virol.* 77:10488-10503.
- Nakajima, K., Maeno, Y., Fukudome, M., Fukuda, Y., Tanaka, S. and Sorimachi, M. 1995. Immunofluorescence test for the rapid diagnosis of red sea bream *iridovirus* infection using monoclonal antibody. *Fish Path.* 30:115-119.
- Oshima, S., Hata, J., Hirasawa, N., Ohtaka, T., Hirono, I., Aoki, T. and Yamashita, S. 1998. Rapid diagnosis of red sea bream iridovirus infection using the polymerase chain reaction. *Dis. Aquat. Org.* 32:87-90.
- Oshima, S., Hata, J., Segawa, C., Hirasawa, N. and Yamashita, S. 1996. A method for direct DNA amplification of uncharacterized DNA viruses and for development of a viral polymerase chain reaction assay: application to the red sea bream iridovirus. *Anal. Biochem.* 242:15-19.

- Qin, Q. W., Chang, S. F., Ngoh-Lim, G. H., Gibson-Kueh, S., Shi, C. and Lam, T. J. 2003. Characterization of a novel ranavirus isolated from grouper *Epinephelus tauvina*. *Dis. Aquat. Org.* 53:1-9.
- Qin, Q. W., Shi, C., Gin, K. Y. and Lam, T. J. 2002. Antigenic characterization of a marine fish iridovirus from grouper, *Epinephelus* spp. *J. Virol. Methods* 106:89-96.
- Reed, L. J. and Muench, H. 1938. A simple method of estimating fifty percent end points. *Am. J. Hyg.* 27:493-497.
- Schnitzler, P. and Darai, G. 1993. Identification of the gene encoding the major capsid protein of fish lymphocystis disease virus. *J. Gen. Virol.* 74:2143-2150.
- Tidona, C. A., Schnitzler, P., Kehm, R. and Darai, G. 1998. Is the major capsid protein of iridoviruses a suitable target for the study of viral evolution? *Virus Genes* 16:59-66.
- Tsai, J. M., Wang, H. C., Leu, J. H., Hsiao, H. H., Wang, A. H., Kou, G. H. and Lo, C. F. 2004. Genomic and proteomic analysis of thirty-nine structural proteins of shrimp white spot syndrome virus. *J. Virol.* 78:11360-11370.
- Wang, C. S., Shih, H. H., Ku, C. C. and Chen, S. N. 2003. Studies on epizootic iridovirus infection among red sea bream, *Pagrus major* (Temminck & Schlegel), cultured in Taiwan. *J. Fish Dis.* 26:127-133.
- Williams, T. 1996. The iridoviruses. *Adv. Virus Res.* 46:345-412.
- Ye, R. W., Wang, T., Bedzyk, L. and Croker, K. M. 2001. Applications of DNA microarrays in microbial systems. *J. Microbiol. Methods* 47:257-272.